A NEW CAVITATING PUMP ROTORDYNAMIC TEST FACILITY

Emilio Rapposelli[**], Angelo Cervone[‡] and Luca d'Agostino[*],

Università di Pisa, 56126 Pisa, Italy

Abstract

The present paper illustrates the operational characteristics of the CPRTF (Cavitating Pump Rotordynamic Test Facility), an experimental apparatus specifically designed for the measurement of rotordynamic fluid forces acting on turbopump impellers in fluid dynamic and inertial/thermal cavitation similarity conditions. The realization of the CPRTF is currently in progress under ASI (Agenzia Spaziale Italiana) funding and consists in the upgrade of the CPTF (Cavitating Pump Test Facility), already available at Centrospazio, Consorzio Pisa Ricerche, Pisa, Italy. The experimental apparatus, operating in water, will be capable of carrying out the measurement of the steady and unsteady forces exerted by the flow on the impellers of cavitating/noncavitating turbopumps. More generally, the facility is designed as a flexible, versatile and inexpensive apparatus that can be readily be adapted to carry out detailed experimental investigations on practically any kind of fluid dynamic phenomena relevant to high performance turbopumps.

The main operational requirements, development choices and design trade-offs that led to the final configuration of the facility are illustrated and its performance in testing of cavitating/noncavitating turbopumps under fluid dynamic and thermal cavitation similarity are discussed. Experimental results from a number of turbopump configurations and operational conditions are presented to illustrate the present capabilities of the facility.

Nomenclature

Latin symbols

b	blade height
d_S	specific diameter
e	whirl eccentricity
F	force
m	mass
M	moment
p	pressure
P	power
$\dot{Q}$	volumetric flow rate
r	radial coordinate
R	electrical resistance
Re	Reynolds number
T	temperature
x, y	lateral coordinates
z	axial coordinate

Greek symbols

ν	kinematic viscosity
ρ	density
σ	Euler cavitation number
ϕ	flow coefficient
ψ	head coefficient
Ω	shaft rotational speed
Ω_S	pump specific speed
Ω_{SS}	suction specific speed

Subscripts

H	hub
t	total
T	tip
V	vapor
1	pump inlet station
2	pump outlet station

Introduction

Propellant feed turbopumps are a crucial component of all primary propulsion concepts powered by liquid propellant rocket engines because of the severe limitations associated with the design of high power density, dynamically stable machines capable of meeting the extremely demanding suction, pumping and reliability requirements of space transportation systems. The recent fatigue failure of an inducer blade due to fluid dynamic instabilities of the LE-7 liquid

[**] Ph.D Student, Department of Aerospace Engineering, Member ASME

[‡] Ph.D Student, Department of Aerospace Engineering

[*] Professor, Department of Aerospace Engineering, Member AIAA

Hydrogen turbopump (NASDA Report No. 94, May 2000, NASDA Report No. 96, June 2000) and the consequent catastrophic loss of the rocket in November 1999 dramatically confirmed that the combined effects of rotordynamic fluid forces and cavitation represent the dominant fluid mechanical phenomena that adversely affect the dynamic stability and pumping performance of high power density turbopumps (Brennen, 1994). The most critical rotordynamic instability in turbopumps is the development of self-sustained lateral motions (whirl) of the impeller under the action of destabilizing forces of mechanical or fluid dynamic origin. Because of their greater complexity, rotordynamic fluid forces have so far received relatively little attention in the open literature, despite of their well recognized potential for promoting rotordynamic instabilities of high performance turbopumps (Rosenmann 1965) and for significantly modifying, in conjunction with cavitation, the dynamic properties of the impeller, and therefore the critical speeds of the whole machine (Jery et al. 1985; Franz 1989; Bhattacharyya 1994; d'Auria, d'Agostino & Brennen 1995; d'Agostino & d'Auria 1997; d'Agostino, d'Auria & Brennen 1998; d'Agostino & Venturini-Autieri 2002; Rapposelli, Falorni & d'Agostino 2002).

Cavitation is the major source of degradation of the suction performance, reliability, power density and useful life of turbopumps, and the cause of other equally undesirable effects such as the reduction of the overall efficiency and the drastic increase of the noise generation (Stripling & Acosta, 1962). Even more importantly for space applications, cavitation can provide the necessary flow excitation, compliance and load-dependence for triggering dangerous rotordynamic and/or fluid mechanic instabilities of the turbopump (Sack & Nottage, 1965; Natanzon et al., 1974; Brennen & Acosta, 1973, 1976; Ng & Brennen, 1978; Braisted & Brennen, 1980; d'Auria, d'Agostino & Brennen, 1994, 1995; d'Agostino & d'Auria 1997; d'Agostino & Venturini-Autieri 2002), or even, through the coupling with thrust generation, of the entire propulsion system (POGO auto-oscillations of liquid propellant rockets, Rubin, 1966).

Brennen (1994) identifies three types of unstable flow phenomena in turbopumps: global flow oscillations (rotating cavitation, surge, partial cavitation and unstable supercavitation), local flow oscillations (blade flutter by rotor-stator interactions or vortex decay), and rotordynamic fluid forces (caused by whirl motions and azimuthal nonuniformities of the flow). Rotating cavitation is the most frequent and potentially dangerous form of turbopump fluid dynamic instability. Just like rotating stall in compressors, the cavitation region depends on the blade angle of attack and propagates from blade to blade, usually at moderately subsynchronous or supersynchronous speeds in the direction of rotation of the inducer. The occurrence of rotating cavitation has been extensively reported in the development of most high performance liquid propellant rocket fuel feed systems, including the Space Shuttle Main Engine (Ryan et al. 1994), the Ariane 5 engine (Goirand et al. 1992) and the LE-7 engine (Kamijo, Yoshida & Tsujimoto 1993). Unacceptable vibrations and blade loads due to rotating cavitation in the inducer have been frequently experienced even at design flow rate well within the operational range of the pump's cavitation number (Hashimoto et al. 1997a, Kamijo, Shimura & Tsujimoto 1993, Tsujimoto, Yoshida Hashimoto 1997). More recently, the analysis of the LE-7 engine identified rotating cavitation and flow pressure oscillations as the causes of the fatigue failure of the inducer blades of the liquid Hydrogen turbopump (NASDA Report No. 96, June 2000). The latest modifications of the SSME (Space Shuttle Main Engine) have also resulted in dangerously higher levels of rotating cavitation in the LOX low pressure turbopumps.

Nowadays, experimentation still plays an essential role for technology progress of high performance turbopumps, because the extreme complexity and imperfect understanding of the relevant unsteady fluid dynamic phenomena prevents the possibility of relying on theoretical or numerical predictions alone. Operational and economic limitations clearly indicate that detailed experiments can only be effectively carried out on scaled turbopump models under fluid dynamic and thermal cavitation similarity. In recognition of these aspects, ASI has funded the realization of the Cavitating Pump Rotordynamic Test Facility (CPRTF), the first openly documented facility in Europe – and one of the few in the world – capable of carrying out the direct measurement of the unsteady rotordynamic fluid forces on scaled cavitating or noncavitating turbopumps.

Experimental Apparatus

The main purpose of the proposed facility is the analysis of steady and unsteady fluid forces and moments acting on the impeller as a consequence of its whirl motion under cavitating or fully-wetted flow conditions, with special emphasis on the onset and development of lateral rotordynamic instabilities. The analysis of whirl phenomena and rotordynamic instabilities can conceivably be accomplished either in a free or in a forced vibration experiment. Actual

rotordynamic destabilization of a turbopump according to the former approach – although more appealing from the standpoint of realism – is not practically feasible in a laboratory environment (apart from safety and economic considerations) due to the large power densities that would be required and the impossibility of simultaneously scaling geometric, kinematic, structural and fluid properties of the turbomachine to preserve structural and fluid dynamic similarity. It is therefore necessary to experimentally reproduce the whirl motion under carefully controlled conditions and measure the impeller forces in a forced vibration experiment. The actual lateral whirl motion of pump impellers is quite complex and so far unpredictable. It is, however, expressible by a Fourier integral and represents a small perturbation of the nominal flow field, so that linear superposition can reasonably be assumed to hold, as confirmed by previous analyses (Adkins & Brennen 1988; d'Auria, d'Agostino & Brennen 1995; d'Auria & d'Agostino 1997; d'Agostino, d'Auria & Brennen 1998; d'Agostino & Venturini-Autieri 2002). Under this assumption, both free and forced vibration experiments would clearly yield equivalent results. These considerations naturally lead to experiments where the effects of individual harmonic components of the impeller whirl motion of given amplitude and angular frequency are separately analyzed. This is conceivably done by imparting to the impeller a whirl motion of given constant eccentricity and angular frequency and measuring the resulting fluid forces on the impeller in the rotating frame. Assuming small eccentricities, the perturbation nature of the whirl motion can be exploited to solve a classical forced vibration problem, where the actual rotordynamic forces on pump prototypes are obtained from the experimental results on scaled models by means of Fourier synthesis and fluid dynamic similarity.

The implications of the inevitable trade-offs between operational requirements and practical limitations on the configuration of the facility have been investigated in depth (d'Auria 1996). The results clearly demonstrated the possibility of designing an experimental apparatus whose operational envelope in terms of specific speed and diameter covers the full range of typical rocket propellant feed turbopumps. In addition, with the proposed choice of the operational parameters (pump speed, pressure rise and impeller size), thermal cavitation similarity of cryogenic propellants is attained with water temperatures well below the boiling point and Reynolds numbers safely in excess of minimum value (one million based on the blade tip speed and radius) typically required for turbulent scaling.

The general configuration of the system is rather strictly constrained by its operational requirements. Adjustable water pressure and temperature over relatively wide ranges, both above and below room conditions, are indispensable for controlling the extent and type (gaseous or vaporous) of cavitation. These are essential features for realistic simulation of turbopumps operating with fluids close to the saturation line, as commonly found in space propulsion applications. Together with the need of controlling cavitation nucleation and hardware corrosion by proper water treatment and additives, the above considerations virtually impose the choice of a closed, recirculating water loop with temperature, pressure, water quality, flow rate, rotation and eccentric whirl controls necessary for the pump to be tested under adjustable flux, load, speed, whirl and cavitation conditions.

The main subsystems of the water loop (Figures 1 and 2) are:

- the pump, contained in an instrumented housing (test section) and driven by a main motor;
- the rotating dynamometer, suspending the pump impeller, for the measurement of the rotor forces;

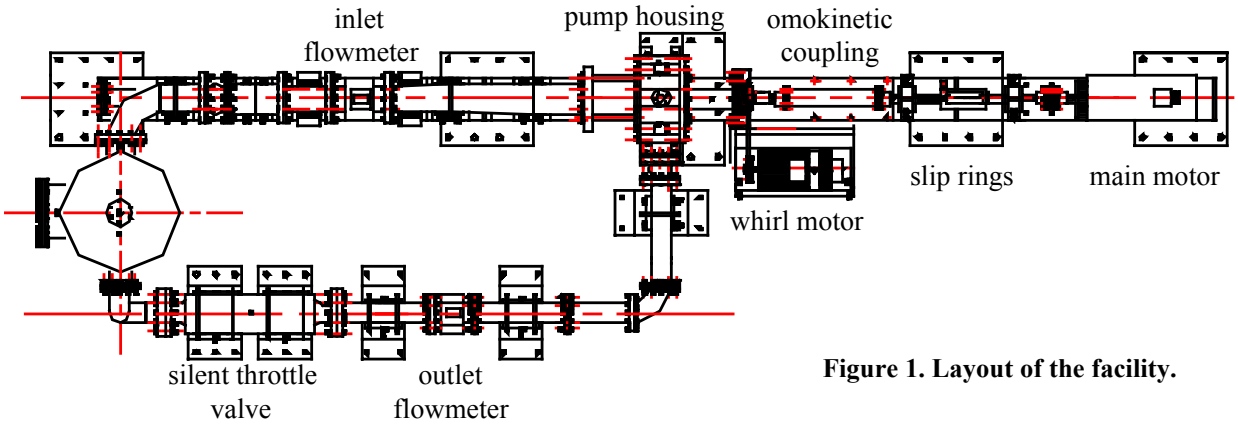

Figure 1. Layout of the facility.

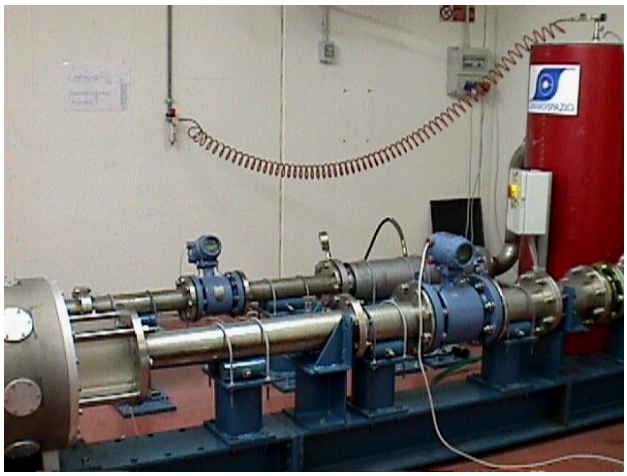

Figure 2. Overview of the test facility.

- the eccentric drive mechanism, driven by an auxiliary motor, for imparting the required whirl motion to the pump impeller;
- the slip ring assembly, for electric connections between rotating elements and the laboratory environment;
- the silent throttle valve, for varying the pump load;
- the inlet and outlet flowmeters, for flow rate measurements;
- the heat exchanger and air bag, for temperature and pressure control and inlet/outlet flow.

Flow fluctuators can also be added at the inlet and outlet of the air bag to generate controlled periodic flow perturbations for studying the dynamic behavior of the pump under unsteady excitation (auto-oscillations). The loop is completed by the supporting structure and piping, the pressurization/depressurization system, the instrumentation and its electronics, the data acquisition and reduction system, and the main and whirl motor controllers.

The eccentric drive mechanism (Figure 3) generates the impeller whirl motion of given eccentricity and angular speed. The pump shaft, driven by the main motor through two omokinetic couplings, is supported eccentrically and the whirl orbit is described by driving the shaft mount at the desired angular speed about the stator axis by means of an auxiliary motor. For rotordynamic studies the whirl motion must be closely tied to the pump rotation and therefore the eccentric drive must be connected, either mechanically or electrically, to the main motor. The electrical connection has been chosen here – in spite of its greater complexity – because of its superior flexibility in continuously varying the whirl motion over a wide range of rotational speeds.

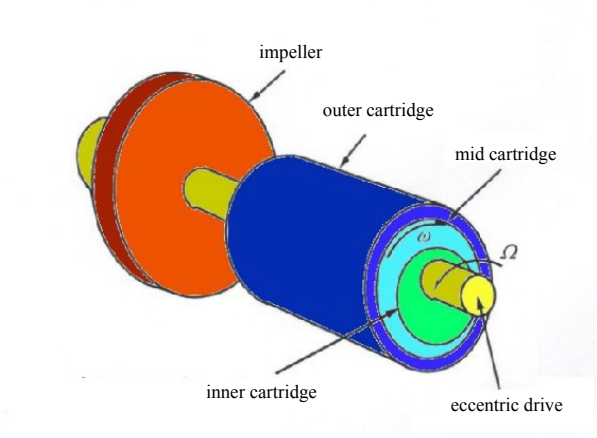

Figure 3. Schematic of the eccentric drive mechanism

For additional flexibility, the facility has been designed and can be implemented in two configurations of increasing complexity and capabilities:

- The Cavitating Pump Test Facility (CPTF), designed for general experimentation on cavitating/non-cavitating turbopumps under thermal and fluid dynamic similarity and specifically for pumping and suction performance tests. This configuration has been completed in June 2001.
- The Cavitating Pump Rotordynamic Test Facility (CPRTF), an upgraded version of the CPTF also capable of investigating rotordynamic fluid forces in forced vibration experiments on turbopumps with rotors of adjustable eccentricity and sub-synchronous or super-synchronous whirl speed. This configuration is now being realized and will be completed by October 2002.

The CPTF does not include the rotating dynamometer, the eccentric drive mechanism and the related motor, transmission, controls and sensors, which are collectively indicated as the Rotordynamic Force Test Facility (RFTF). Since no synchronization of the angular rotations of the two shaft is needed, from the kinematic point of view it is sufficient to simply control the angular velocity of the main shaft. The motor controls and the data acquisition system are therefore simpler, although their general architecture remains unchanged.

The CPRTF, on the other hand, also includes the RFTF. Its motor controls and the data acquisition system are somewhat more complex, because its is necessary to synchronize the two shafts and assure that the impeller angular position repeats with identical kinematic features after an integer number of whirl

orbits, in order to obtain a truly periodic phenomenon over a intervals multiple of the rotational and whirl periods. This requirement is imposed by the need of averaging a large number of repetition cycles in order to extract the information on the average effects of the flow on the rotordynamic fluid forces along the impeller whirl orbit, rejecting the fluctuations due to turbulence and the occurrence of individual cavitation events.

Besides, with just minor modifications the facility can readily be adapted for virtually any kind of experimental investigations on fluid dynamic phenomena of immediate relevance to the performance and stability of turbopumps for liquid propellant rocket propulsion applications.

Component Characteristics

Water Loop Hardware

- The supporting structure, essentially consisting of an I-beam, rigidly connected to the laboratory floor by means of chemical bolts and to a series of adjustable mounts for the pump housing, the motors and the loop pipes.
- The 500 l air bag and heat exchanger, with a 5 kW electrical heater and a 40 l air bladder, which can vary the water temperature of the loop from room conditions to near the boiling point (90 °C) and the suction pressure from 5 bar to 1000 Pa above the saturation value.
- The suction and discharge piping, realized in 316 stainless steel, with maximum pressures of 5 and 10 bar and nominal diameters of 6 and 4 inches, respectively. The line just upstream of the test section can be easily adapted to the inlet pump diameter or substituted with a small hydrodynamic tunnel for carrying out experiments in thermal/inertial cavitation conditions.
- A series of auxiliary lines and tanks, necessary for emptying or filling and pressurizing or depressurizing the loop.
- Two flow straighteners on the suction and discharge lines, to reduce the large scale flow nonuniformity and turbulence for precise operation of the flowmeters and control of the inlet flow to the pump.
- Two elastic couplings on the suction and discharge lines, to allow for vibration insulation, misalignment compensation and easy access and/or reconfiguration of the pump.
- A two-stage silent throttle valve, special item from Innerspace Corp., on the pump discharge line, used to adjust the pump load without generating internal cavitation and therefore without introducing spurious dynamic excitation and additional cavitation nuclei in the flow.

Motors and Transmissions

- The main motor, MOOG mod. FASF3V8029, brushless, 6-poles, 30 kW maximum power, 100 Nm maximum torque, $\Omega = 0 \div 3000$ rpm controlled speed, $3000 \div 6000$ rpm maximum uncontrolled overspeed on the maximum power line. The main motor is controlled by its power electronics in both angular position and velocity with errors less than ±1° and ±3 rpm. The motor controller can be digitally programmed via PC code and interface for carrying out complex rotation histories. It also generates digital readouts of the shaft angular position, rotational speed and torque for the data acquisition system.
- The whirl motor, MOOG mod. FASF2V4030, brushless, 6-poles, 5.6 kW maximum power, 18 Nm maximum torque, $\omega = 0, \pm 3000$ rpm controlled speed. The whirl motor is controlled by its power electronics in angular position and velocity with reference to the main motor, in order to retain a specified velocity ratio ω/Ω and initial/final angular positions during test runs. The motor controller also generates digital readouts of the angular position and rotational speed of the eccentricity for the data acquisition system.
- Two omokinetic couplings, allowing for the rotor eccentricity and transferring the rotational motion from the main motor to the pump shaft.
- The slip ring assembly, Fabricast mod. 4200-1.498-42-36U, 64 leads, necessary to effect with the necessary accuracy and stability the electrical connections between the instrumented rotor (rotating dynamometer or other impeller-mounted sensors) and the stationary electronics (exciters, amplifiers and data acquisition).
- The eccentric drive mechanism, schematically illustrated in Figure 3. It consists in the combination of two inner/outer cylindrical mounts, each with 1 mm fixed eccentricity. The inner mount internally supports the pump shaft. The outer mount is externally supported by the pump stator. Before each run the relative angle of the two eccentricities can be finely adjusted and fixed between 0° and 180°, realizing a total shaft eccentricity varying from 0 to 2 mm. The whole group (and the pump shaft with it) is driven by the auxiliary motor at the whirl speed about the geometric axis of the pump stator. High-precision roller bearings (pump side) and oblique ball

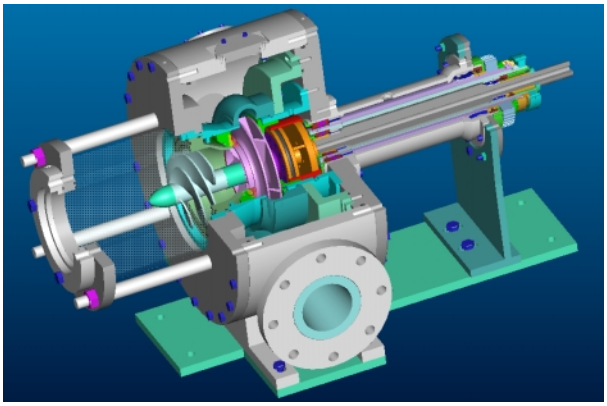

Figure 4. CPRTF test section assembly.

bearings (drive side) are used in order to finely control the shaft position, to assure smooth running, and to attain the required rotation and whirl speeds (3000 rpm) with grease lubrication. Considerably higher speeds (about 6000 rpm) can be reached with oil lubrication. Significant attention has been paid in the selection and integration of the radial seals insulating the bearings from the water on the side facing the pressurized pump housing.

Test Section Assembly

- The test section (Figure 4), comprising the pump housing (Figure 5), and the transparent inducer casing (Figure 6). The pump housing essentially consists in a hollow aluminum cylinder rigidly mounted on the supporting structure and closed by two lids. The rear lid internally supports the pump and is externally connected to the mechanism driving the shaft. The front lid is connected with the transparent inlet duct and provides access to the pump assembly for mounting/dismounting and reconfiguration operations. The internal dimensions of the housing (500 mm ID, 281 mm axial length) and its 11 bar maximum rated pressure allow for accommodation of a wide range of full-scale turbopumps for liquid propellant feed systems. In the CPRTF configuration, 0.1–0.7 mm adjustable gap axial labyrinths provide flow sealing at the inlet and outlet stations of the pump. Leakage flow is recirculated to the pump inlet. The housing pressure is kept near the discharge value in order to minimize volute stresses and allow for the use of low strength materials. Control of the axial thrust can be obtained by suitable choice of the radial location of the face seals. The transparent inlet duct, realized in Plexiglas with exchangeable inner liner to accommodate pumps and/or inducers

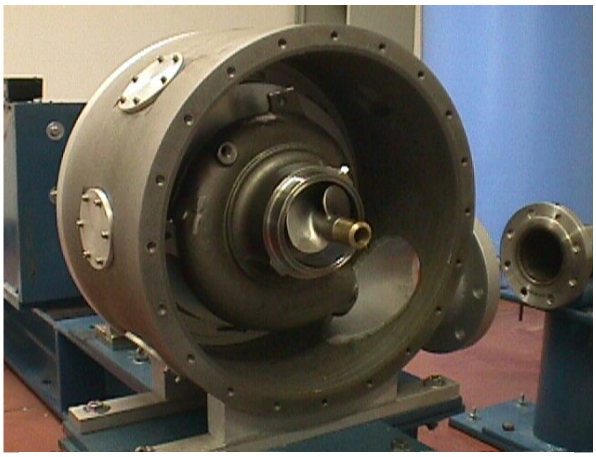

Figure 5. CPRTF test section.

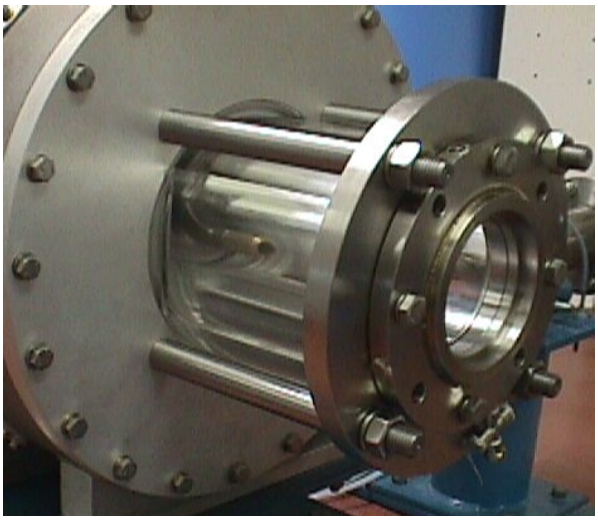

Figure 6. Inlet of the CPRTF test section.

with diameters up to 200 mm, allows for optical access to the inlet flow with nearly matched (nondistorting) optical interfaces.

- The rotating dynamometer is schematically illustrated in Figure 7. It is realized in just one piece of phase hardening steel AISI PH 17-4 and comprises two flanges connected by four square cross-section posts acting as flexing elements. Their deformation is sensed by 40 semiconductor strain gauges (Micron, mod. SS-060-033-1000P-S4, 1000 Ω, 155 gauge factor) arranged in 10 full bridges, which provide redundant measurements of the forces and moments acting on the impeller. Each bridge is temperature self-compensated and, for increased precision, has separate bipolar excitation and read-out. The temperature dependence of the gauge factors is accounted for in the data reduction process. The sizing of the sensing posts trades off sensitivity against

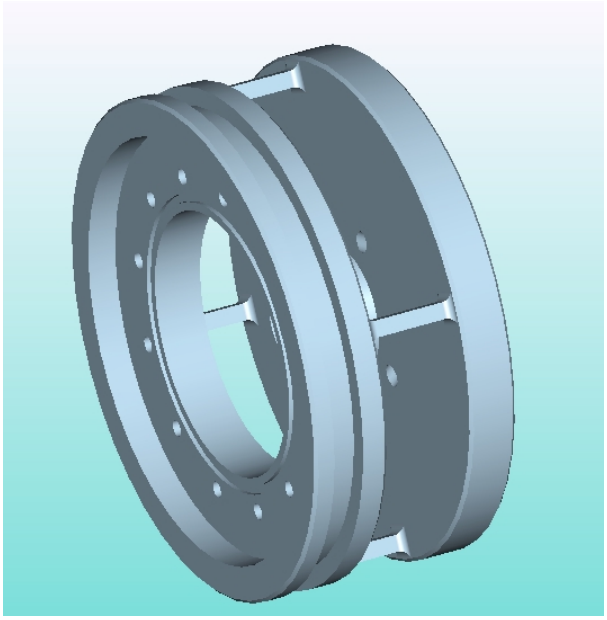

Figure 7. Rotating dynamometer.

structural resistance, operational stability and position control (stiffness). The current design of the dynamometer is optimized for a suspended mass of 4 kg with 70 mm gyration radius, an added mass on the order of 2 kg (based on the expected magnitude of the rotordynamic forces), a rotational speed of 3000 rpm in the absence of eccentricity, and maximum rotational and whirl speeds up to 2000 rpm with 2 mm shaft eccentricity. The torsional and flexing critical speeds of the impeller are about one order of magnitude higher that the rotational speed in order to minimize the gain (±2%) and phase errors (±3°) of the force measurements.

Instrumentation and Data Acquisition

- Two electromagnetic flowmeters, mod. 8705 by Fisher-Rosemount, mounted on the suction and discharge lines for the instantaneous measurement of the pump's inlet/outlet flow rates (0 to 100 l/s).
- An absolute pressure transducer, Druck mod. PMP 1400, 0–1 bar, 0.15% class, on the inlet line to the pump for monitoring the suction pressure.
- A differential pressure transducer, Kulite mod. BMD 1P 1500 100, 0–100 psid, 0.1% class, mounted across the inlet and outlet lines for monitoring the pump pressure raise.
- A medium-speed data acquisition system, based on an 16-channel signal conditioning board National Instruments mod. SCXI 1520 and a 250 kS/s acquisition board National Instruments mod. 6024E, used for the suction/discharge pressures and flow rates, the rotational and whirl speeds and the water temperature.
- A high-speed data acquisition system based on two 8-channel signal conditioning boards National Instruments mod. SCXI 1520 and a 32 channel 1.25 MS/s National Instruments board mod. 6071E, used for the excitation, conditioning and acquisition of the rotating dynamometer and/or other fast instrumentation.

Table 1. CPTF operational characteristics

Pump rotational speed	$\Omega = 0 \div 3000$ rpm
Main motor power	$P \le 30$ kW
Main motor torque	$M \le 100$ Nm
Suction pressure	$p_{t1} = 0.01 \div 6$ bar
Discharge pressure	$p_{t2} \le 11$ bar
Volumetric flow rate	$\dot{Q} \le 0.1$ m^3/s
Flow temperature	$T = 10 \div 90$ °C
Suction line diameter	DN = 6"
Discharge line diameter	DN = 4"
Impeller eye radius	$r_{T1} \le 90$ mm
Impeller outlet radius	$r_{T2} \le 112$ mm
Impeller outlet width	$b_2 \le 30$ mm

Table 2. RFTF operational characteristics

Adjustable eccentricity	$e = 0 \div 2$ mm
Whirl rotational speed	$\omega = -3000 \div 3000$ rpm
Nominal suspended mass	$m_S = 4$ kg
Dynamometer loads:	
lateral	$F_x = F_y \le 2400$ N
axial	$F_z \le 15000$ N
bending	$M_x = M_y \le 1400$ Nm
torque	$M_z \le 400$ Nm

CPRTF Operational Envelope

The operational characteristics of the facility have been chosen accounting for the need of retaining fluid dynamic and thermal cavitation similarity for accurate scaling of actual turbopumps, while still meeting stringent versatility, economic, maintenance and safety requirements. Fluid dynamic similarity requires that the full-scale prototype and the test model have equal shape, specific speed and cavitation number (Euler cavitation scaling), and equal Reynolds number (viscous and turbulent scaling). For thermal cavitation similarity, in both machines the time for a nucleus to develop thermally-controlled growth must be in the same ratio to its residence time in the turbopump. Since pump prototypes typically run at Reynolds numbers $\mathrm{Re} = 2\,\Omega r_{T2}^2 / \nu$ exceeding ten million, strict application of viscous and turbulent scaling leads to unacceptably high values of the speed and power of the model pump

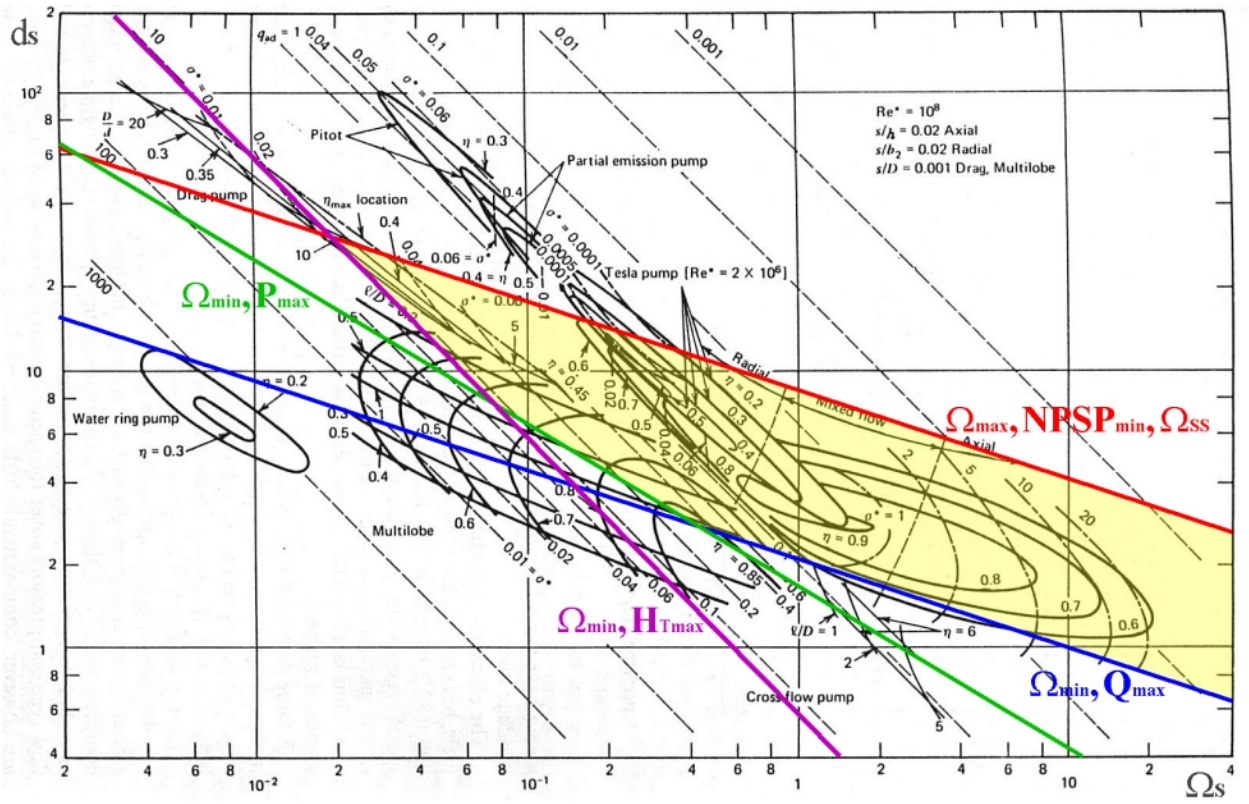

Figure 8. The CPRTF operational envelope. The accessible combinations of specific speeds and diameters $\Omega_S\ d_S$ are simultaneously internal to the lines corresponding to the operational constraints.

and, consequently, to equivalent water temperatures for thermal cavitation scaling far exceeding the boiling point. Luckily, however, Reynolds scaling is practically constant for $\mathrm{Re} > 10^6$, when the flow in the pump is fully turbulent. By exploiting this situation, the speed, power and equivalent water temperature for thermal cavitation scaling of the model pump in the CPRTF can be reduced within acceptable values (below the boiling point) without significant degradation of the representativeness of the tests, thereby preserving the capability of realistically reproducing the actual operation of full-scale machines.

The main operational parameters of the CPTF and RFTF are summarized in Tables 1 and 2. The resulting operational envelope of the CPRTF in terms of the nominal specific speed, Ω_{SS}, and diameter, d_S, of the machine is shown in Figure 8, and covers with ample margins the parametric space occupied by axial, mixed, and radial flow turbopumps typically used in rocket propellant feed systems. Similarly, the equivalent water temperature of a full-scale machine tested in the CPRTF at $\mathrm{Re} = 10^6$ is shown in Figure 9 as a function of the actual Reynolds number of the same machine operating with a number of common space propellants. The results confirm that thermal cavitation similarity in the CPRTF is attained at water temperatures safely lower than the boiling point.

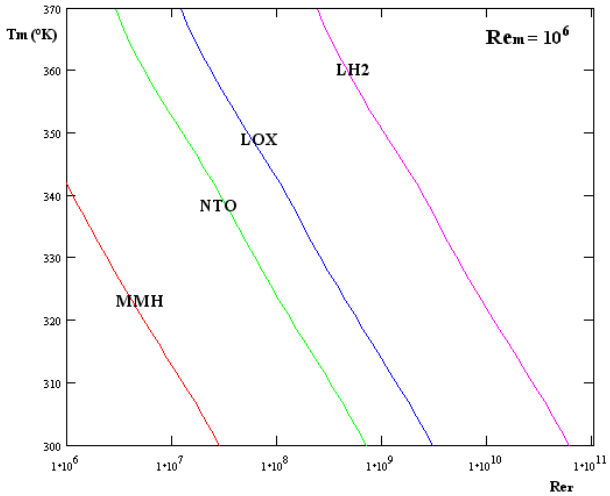

Figure 9. Equivalent water temperature T_m in the CPRTF for scaling a pump operating with different propellants at a Reynolds number $\mathrm{Re}_r = 2\,\Omega r_T^2/\nu$. The Reynolds number of the pump in the CPRTF is $\mathrm{Re}_m = 10^6$.

Figure 10. Axial inducer and impeller of the test pump used for CPTF validation.

Demonstration Tests

In the following some of the experimental results obtained during the CPTF validation with a commercial pump shown in Figure 10 are reported. The characteristic curves obtained for the complete pump (inducer and centrifugal impeller) are presented in Figure 11. In particular, the two curves respectively represent the behavior of the work coefficient $\psi = \left(p_{t2} - p_{t1}\right) \Big/ \rho \Omega^2 r_{T2}^2$ and the efficiency η of the machine as functions of the flow coefficient $\phi = \dot{Q} \Big/ \pi \Omega r_{T1}^3$. Figure 12 shows the cavitation characteristics of the test pump as a function of the Euler number $\sigma = \left(p_1 - p_V\right) \Big/ \frac{1}{2} \rho A \Omega^2 r_{T1}^2$ for $\phi = 0.222$, and illustrates the influence of thermal cavitation effects on the suction capabilities of the reference inducer. As expected, cavitation breakdown is delayed at higher values of the water temperature and the work coefficient increases slightly. A picture of the heavily cavitating flow in the test inducer near breakdown conditions is illustrated in Figure 13.

Surge and rotating cavitation in the turbopump can readily be detected in the CPTF and CPRTF either by optical means or by monitoring the inlet pressure and flow rate to the inducer. The CPRTF data acquisition includes low-pass anti-aliasing filters of adjustable cut-off frequency on all input channels for accurate numerical evaluation of the signal spectra. Figure 14 shows a typical trace of the flow pressure just upstream of the inducer inlet section under heavy surge conditions. An example of the pressure spectrum at several values of the cavitation number is displayed in Figure 15. Discrimination of cavitation surge from rotating cavitation and other unsteady flow phenomena is readily and efficiently effected by cross-correlation of the inlet pressure and flow rate.

Conclusions

The present activity is concerned with the realization of the CPRTF, an economic and easily

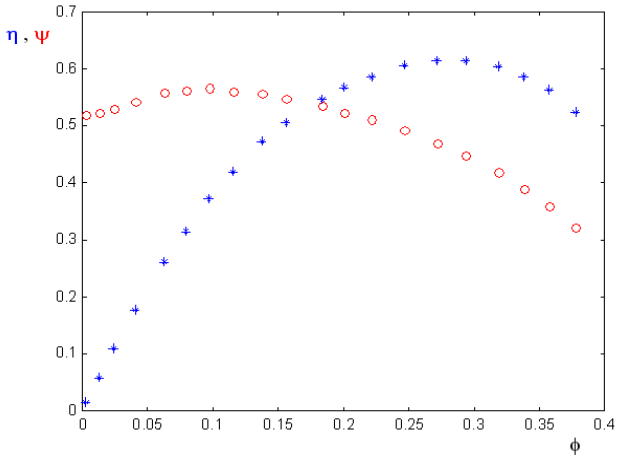

Figure 11. Head coefficient (circles) and efficiency (crosses) of the CPTF test pump (impeller with inducer) as functions of the flow coefficient.

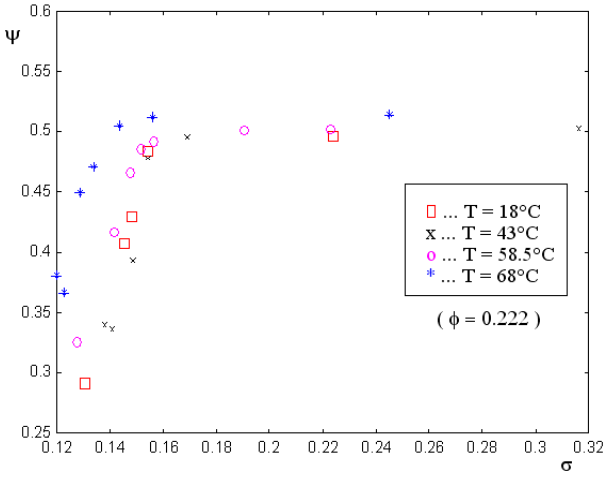

Figure 12. Thermal cavitation effects on the suction characteristics of a three-bladed helical inducer ($\beta_T = 18°$, $r_T = 60$ mm, $r_H = 22$ mm) in water at $\mathrm{Re} = 2\Omega r_T^2 / \nu_L = 10^6$ and several temperatures.

Figure 13. Extensive cavitation in the test inducer.

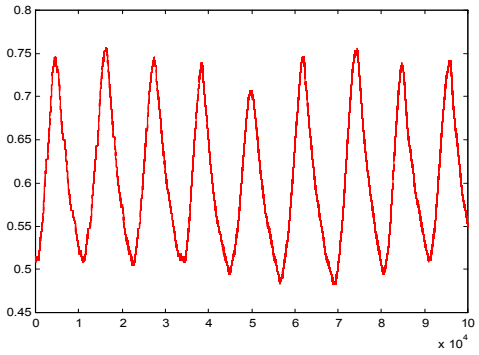

Figure 14. Typical inlet pressure signal under extensive surge conditions in the test inducer.

reconfigurable water-loop facility for fluid mechanic and rotordynamic tests on scaled turbopumps under cavitating or noncavitating conditions. The facility is especially intended for the direct measurement of rotordynamic and cavitation fluid forces on the rotating elements and/or for experimentation on virtually any kind of fluid dynamic phenomena relevant to high performance turbopumps. Together with a similar rig at Caltech, the CPRTF is the only openly documented facility that combines the capabilities of measuring the instantaneous fluid loads on the impellers with proper scaling of thermal cavitation effects in an easily-instrumentable test environment, suitable for detailed and economic experimentation on the full-scale turbopumps used in liquid propellant rocket feed systems.

The CPRTF represents therefore an effective support tool in the turbopump design, and is clearly complementary to more expensive and lightly instrumented industrial test facilities that are primarily devoted to the final certification of established designs. Ultimately, it will give the designers of high performance turbopumps a deeper insight on the development of dangerous flow instabilities of crucial importance in rocket propulsion applications. In more practical terms, CPRTF test results will provide experimental data on the dependence of the onset, form and extent of cavitation-induced instabilities on the scaling parameters describing the operational conditions of the machine and the intensity of thermal effects, which commonly occur in most cryogenic propellants. By proper extrapolation based on well-established similarity laws, this information will allow for realistic predictions of these phenomena to be made in actual rocket engine turbopunps, thereby effectively contributing to identify the operational regimes that are likely to develop into dangerous and potentially destructive fluid dynamic instabilities.

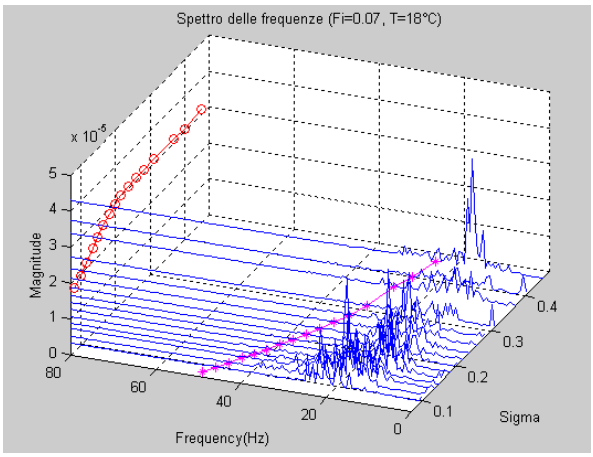

Figure 15. Typical waterfall plot of the inlet pressure spectra in the test inducer for several values of the cavitation number.

By specifically addressing the performance and stability issues raised by the European Space Agency in connection with the initiation of practical work on high power density turbopumps in the context of the first phase of the FESTIP Program, the realization of the CPRTF is fully coherent with the current involvement of the Italian and European industry in the space sector and there are reasons to believe that it will usefully to the development and demonstration of the high specific performance technologies required by the primary propulsion systems of future reusable launchers.

Acknowledgements

The present work has been partially supported by the European Space Agency under the FESTIP-1 contract No. 11.482/95/NL/FG and by the Agenzia Spaziale Italiana under the 1998 and 1999 contracts for fundamental research. The authors would like to acknowledge the help of the students Fabrizio d'Auria, Sergio Bondi, Davide Mazzini, Roberto Menoni, Luisella Vigiani, Cristina Bramanti and Andrea Milani who participated to the design of the facility, and express their gratitude to Profs. Mariano Andrenucci and Renzo Lazzeretti of the Dipartimento di Ingegneria Aerospaziale, Università degli Studi di Pisa, Pisa, Italy, for their constant and friendly encouragement.

References

Adkins D.R. and Brennen C.E., 1988, "Analysis of Hydrodynamic Radial Forces on Centrifugal Pump Impeller", *ASME J. Fluids Eng*., Vol. 110, pp. 20-28.

Bhattacharyya A., 1994, "Internal Flows and Force Matrices in Axial Flow Inducers", *Ph. D. thesis, Div. Eng. & Appl. Science, Caltech*, Pasadena, CA, USA.

Braisted D.M. and Brennen C.E., 1980, "Auto-oscillation of Cavitating Inducers", *Polyphase Flow and Transport Technology, ed. R.A. Bajura,* ASME Publ., New York, pp. 157-166.

Brennen C.E., 1994, "Hydrodynamics of Pumps", *Concepts ETI, Inc*. and *Oxford University Press*.

Brennen C.E. and Acosta A.J., 1976, "The Dynamic Transfer Function for a Cavitating Inducer", *ASME J. Fluids Eng*., Vol. 98, pp. 182-191.

Brennen C.E. and Acosta A.J., 1973, "Theoretical, Quasi-Static Analysis of Cavitation Compliance in Turbopumps", *J. Spacecrafts & Rockets*, Vol. 10, No. 3, pp. 175-180.

d'Agostino L., & Venturini-Autieri M., 2002, "Three-Dimensional Analysis of Rotordynamic Fluid Forces on Whirling and Cavitating Finite-Length Inducers", *9th Int. Symp. on Transport Phenomena and Dynamics of Rotating Machinery (ISROMAC-9),* Honolulu, HI, USA, February 10-14.

d'Agostino L. & d'Auria F., 1997, "Three-Dimensional Analysis of Rotordynamic Forces on Whirling and Cavitating Inducers", *ASME FED Summer Meeting*, Vancouver, BC, Canada, June 22-26.

d'Agostino L., d'Auria F. & Brennen C.E., 1998, "A Three-Dimensional Analysis of Rotordynamic Forces on Whirling and Cavitating Helical Inducers", *ASME J. of Fluids Eng.,* Vol. 120, pp. 698-704.

d'Auria F., 1996, "Cavitating Pump Test Facility (WP 2310)", *Technical Note, FESTIP: Technology Developments in Rocket and Air Breathing Propulsion for Reusable Launch Vehicles*, ESTEC Contract No. 11.482/95/NF/FG, Centrospazio, Pisa, Italy, Nov. 28.

d'Auria F., d'Agostino L. & Brennen C.E., 1994, "Linearized Dynamics of Bubbly and Cavitating Flows in Cylindrical Ducts", *ASME FED Summer Meeting, Incline Village*, NV, USA, June 19-23.

d'Auria F., d'Agostino L. & Brennen C.E., 1995, "Bubble Dynamic Effects on the Rotordynamic Forces in Cavitating Inducers", *ASME FED Summer Meeting*, Hilton Island, SC, USA, August 13-18.

Franz R. et al., 1989, "The Rotordynamic Forces on a Centrifugal Pump Impeller in the Presence of Cavitation", *ASME FED-81*, pp. 205-212.

Goirand B., Mertz A.L., Jousselin F. & Rebattet C., 1992, "Experimental Investigations of Radial Loads Induced by Partial Cavitation with Liquid Hydrogen Inducer", *IMechE, C453/056*, pp. 263-269.

Hashimoto T., Yamada H., Funatsu S., Ishimoto J., Kamijo K. & Tsujimoto Y., 1997a, "Rotating Cavitation in Three and Four-Bladed Inducers", *AIAA Paper 97-3026*.

Hashimoto T., Yamada H., Watanabe M., Kamijo K. & Tsujimoto Y., 1997b, "Experimental Study on Rotating Cavitation of Rocket Propellant Pump Inducers", *J. Propulsion and Power*, Vol. 13, No. 4.

Jery B. et al., 1985, "Forces on Centrifugal Pump Impellers", *2nd Int. Pump Symp*., Houston, TX, USA, April 29-May 2, 1985.

Kamijo K., Yoshida M. & Tsujimoto Y., 1993, "Hydraulic and Mechanical Performance of LE-7 LOX Pump Inducer", *ASME J. Propulsion and Power*, Vol. 9, No. 6, pp. 819-826.

Kamijo K., Shimura T. & Tsujimoto Y., 1993, "Experimental and analytical study of rotating cavitation", *ASME FED-190*, pp. 33-43.

NASDA, 2000a, *Report No. 94*, May 2000.

NASDA, 2000b, *Report No. 96*, June 2000.

Natanzon M.S. el al., 1974, "Experimental Investigation of Cavitation Induced Oscillations of Helical Inducers", *Fluid Mech. Soviet Res*., Vol. 3 No. 1, pp.38-45.

Ng S.L. and Brennen C.E., 1978, "Experiments on the Dynamic Behavior of Cavitating Pumps", *ASME J. Fluids Eng*., Vol. 100, No. 2, pp. 166-176.

Rapposelli E., Falorni R. & d'Agostino L., 2002, "Two-Phase and Inertial Effects on the Rotordynamic Forces in Whirling Journal Bearings", *Proc. 2002 ASME FED Summer Meeting*, Montreal, Quebec, Canada, July 14-18.

Rosenmann W., 1965, "Experimental Investigations of Hydrodynamically Induced Shaft Forces with a Three Bladed Inducer", *Proc. ASME Symp. on Cavitation in Fluid Machinery*, pp. 172-195.

Rubin S., 1966, "Longitudinal Instability of Liquid Rockets due to Propulsion Feedback (POGO)", *J. of Spacecraft and Rockets*, Vol.3, No. 8, pp.1188-1195.

Ryan R.S., Gross L.A., Mills D. & Michell P., 1994, "The Space Shuttle Main Engine Liquid Oxygen Pump High-Synchronous Vibration Issue, the Problem, the Resolution Approach, the Solution", *AIAA Paper 94-3153*.

Sack L.E. and Nottage H.B., 1965, "System Oscillations Associated to Cavitating Inducers", *ASME J. Basic Eng*., Vol. 87, pp. 917-924.

Stripling L.B. and Acosta A.J., 1962, "Cavitation in Turbopumps – Part 1, *ASME J. Basic Eng*., Vol. 84, pp. 326-338.

Tsujimoto Y., Yoshida Y., Hashimoto T.,1997, "Observation of Oscillating Cavitation of an Inducers", *ASME J. Fluids Eng.ing*, Vol. 119, pp. 775-781.